PHYSICAL REVIEW C VOLUME 22, NUMBER 5 NOVEMBER 1980

Effect of the nuclear compressibility coefficient on the expansion of compressed nuclear matter

Arnold J. Sierk and J. Rayford Nix
Theoretical Division, Los Alamos Scientific Laboratory, Los Alamos, New Mexico 87545
(Received 11 July 1980)

On the basis of a conventional nonrelativistic fluid-dynamics model, we study the expansion of spherically symmetric nuclear matter that is initially compressed and excited in head-on collisions of equal targets and projectiles at a laboratory bombarding energy per nucleon of 250 MeV. We use a new functional form for the nuclear equation of state which has the property that the speed of sound approaches the speed of light in the limit of infinite compression. For various values of the nuclear compressibility coefficient, the fluid-dynamical equations of motion are solved until the matter expands to a freezeout density at which fluid dynamics ceases to be valid. At this point the remaining thermal energy is superimposed in terms of a Maxwell-Boltzmann distribution with appropriate nuclear temperature. For nonzero values of the compressibility coefficient ranging form 100 to 400 MeV, the energy distribution at the freezeout density of the expanding matter depends slightly upon the compressibility coefficient. However, the final-energy distribution after thermal folding is independent of the compressibility coefficient to within graphical accuracy. For zero compressibility coefficient, which corresponds to the expansion of a perfect gas, the energy distribution is significantly different form that for nonzero compressibility coefficient at the freezeout point, and is slightly different from that for nonzero compressibility coefficient after thermal folding. For both zero and nonzero values of the compressibility coefficient, the final energy distributions are significantly different from a Maxwell-Boltzmann distribution corresponding to entirely thermal energy, and are moderately different from the energy distribution corresponding to the Siemens-Rasmussen approximation.

[NUCLEAR REACTIONS Equal target and projectile, E_{bom}/nucleon = 250 MeV; calculated energy distribution of expanding spherically symmetric nuclear matter. High-energy heavy-ion collisions, nonrelativistic nuclear fluid dynamics, nuclear equation of state, nuclear freezeout, thermal folding with Maxwell-Boltzmann distribution, Siemens-Rasmussen approximation.]

I. INTRODUCTION

High-energy heavy-ion collisions provide a unique opportunity to explore what happens when heavy nuclei become highly compressed and excited. As part of the recent surge of interest in this area, several calculations of high-energy heavy-ion collisions have been performed on the basis of fluid-dynamical models,[1-10] where the basic input is the nuclear equation of state. It is of crucial importance to know the sensitivity of the calculated results to the input equation of state.

Although some two-dimensional and three-dimensional calculations have been performed for different equations of state,[5-8] the fairly large numerical errors that are present have precluded an accurate assessment of this sensitivity. It is our purpose here to study one aspect of this question in a simple, one-dimensional calculation for which an accurate numerical solution is possible. In particular, we study the sensitivity of the energy distribution of expanding spherically symmetric nuclear matter to the nuclear compressibility coefficient.

The particular nuclear equation of state that we use is introduced in Sec. II; it is a new functional form for which the speed of sound approaches the speed of light in the limit of infinite compression. We discuss in Sec. III the fluid-dynamical equations of motion, along with our initial conditions and method of solution. In Sec. IV we calculate the energy distribution of the expanding matter, both at the freezeout density at which fluid dynamics ceases to be valid and after superimposing the remaining thermal energy in terms of a Maxwell-Boltzmann distribution with appropriate nuclear temperature. Our conclusions are presented in Sec. V.

II. NUCLEAR EQUATION OF STATE

The nuclear equation of state, which specifies how the pressure depends upon density and thermal energy, can be written as the sum of a contribution from the compressional energy and a contribution from the thermal energy. This is seen most clearly by recalling that the total internal energy per nucleon is given by[4]

$$\mathcal{E}(n, \mathcal{I}) = \mathcal{E}_0(n) + \mathcal{I} ,$$

where $\mathcal{E}_0(n)$ is the ground-state energy per nucleon at nucleon number density n and $\mathcal{I}$ is the thermal energy per nucleon. The pressure p is then ob-

tained from the fundamental relation[4]

$$p = n^2 \frac{\partial \mathcal{E}(n,s)}{\partial n}\bigg|_s = n^2 \frac{d\mathcal{E}_0(n)}{dn} + n^2 \frac{\partial s}{\partial n}\bigg|_s , \quad (1)$$

with differentiation at constant entropy per nucleon S.

A. Compressional contribution

For the ground-state energy per nucleon $\mathcal{E}_0(n)$ we use a new functional form which has the property that the speed of sound approaches the speed of light in the limit of infinite compression. This is achieved by taking $\mathcal{E}_0(n)$ for n greater than or equal to a critical value n_a to be a parabola in the square root of the density, so that in the limit of infinite compression it increases linearly with density. In the limit of zero density, $\mathcal{E}_0(n)$ is taken to be the difference between a specified term proportional to $n^{2/3}$ that represents the kinetic energy of noninteracting nucleons and a term proportional to n whose coefficient is adjusted so that the two forms join smoothly with continuous value and first derivative.

To be specific, our equation for $\mathcal{E}_0(n)$ is

$$\mathcal{E}_0(n) = \begin{cases} an^{2/3} - bn, & n \leq n_a \\ \mathcal{E}_0(n_0) + \frac{2}{9}K\left[\left(\frac{n}{n_0}\right)^{1/2} - 1\right]^2, & n \geq n_a \end{cases} \quad (2)$$

where

$$a = \frac{3}{10}\left(\frac{3\pi^2}{2}\right)^{2/3}\frac{\hbar^2}{m_0}$$

and m_0 is the nucleon mass, which we take equal to the average of the proton and neutron masses. The quantity

$$K = 9n_0^2\left(\frac{d^2\mathcal{E}_0}{dn^2}\right)_0$$

is the nuclear compressibility coefficient, and

$$n_0 = \frac{1}{(4\pi/3)r_0^3}$$

is the normal nucleon number density. We use

$$r_0 = 1.18 \text{ fm}$$

for the value of the fundamental nuclear-radius constant[11] and

$$\mathcal{E}_0(n_0) = -8 \text{ MeV}$$

to simulate the effects of surface and Coulomb energies for finite nuclei. The critical density n_a is obtained by solving iteratively the equation

$$\tfrac{1}{3}an_a^{2/3} + \frac{2}{9}\frac{K}{n_0^{1/2}}n_a^{1/2} - [\mathcal{E}_0(n_0) + \tfrac{2}{9}K] = 0 .$$

The coefficient b is then given by

$$b = \frac{2}{3}\frac{a}{n_a^{1/3}} + \tfrac{2}{9}K\left[\frac{1}{(n_a n_0)^{1/2}} - \frac{1}{n_0}\right].$$

The resulting ground-state energy $\mathcal{E}_0(n)$ is shown in Fig. 1 for five values of the nuclear compressibility coefficient K ranging from 0 to 400 MeV.

B. Thermal contribution

For the thermal contribution to the pressure we use the nonrelativistic Fermi-gas model, which yields[4]

$$p_{\text{thermal}} = n^2 \frac{\partial s}{\partial n}\bigg|_S = \tfrac{2}{3}ns . \quad (3)$$

Unlike what is often implied, this is a general result for the nonrelativistic Fermi-gas model that is valid to all orders in the temperature.

III. NONRELATIVISTIC SPHERICALLY SYMMETRIC EXPANSION

A. Initial conditions

We consider in this section the head-on collision of an equal target and projectile with laboratory bombarding energy per nucleon of 250 MeV, which corresponds relativistically to a center-of-mass energy per nucleon of 60.53 MeV. We make the

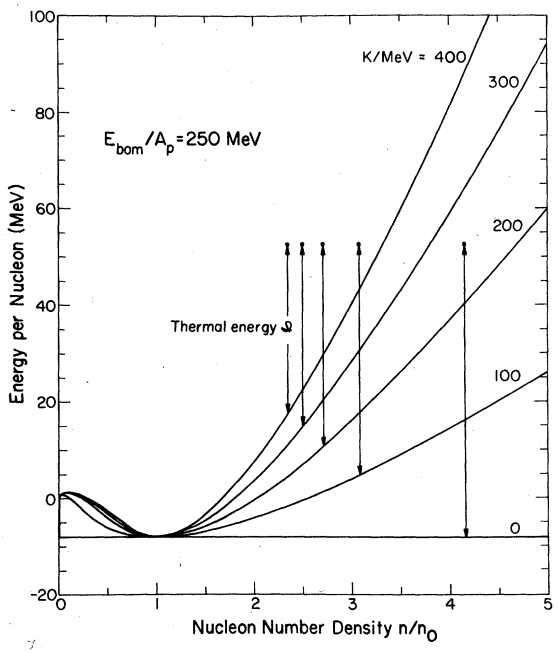

FIG. 1. Compressional contribution to our nuclear equation of state, for five values of the compressibility coefficient K. The arrows denote the thermal energy per nucleon s and the nucleon number density n achieved in the head-on collision of an equal target and projectile with laboratory bombarding energy per nucleon of 250 MeV.

drastic geometrical assumption that during the collision the nuclear matter is uniformly compressed and excited into a sphere at rest in the center-of-mass system, with constant initial values of the density, compressional energy, and thermal energy determined by relativistic Rankine-Hugoniot relations.[4] These relations are obtained by integrating the relativistic equations of fluid dynamics over an infinitesimal volume near the contact point in a head-on collision. The solutions for the cases considered here are illustrated in Fig. 1. With increasing compressibility coefficient, the initial compressional energy per nucleon increases, whereas the initial density and thermal energy per nucleon decrease.

These quantities serve as initial conditions for the spherically symmetric expansion of the matter, which is treated nonrelativistcally in two stages. In the first stage, corresponding to densities greater than a freezeout density, we integrate numerically in one dimension nonrelativistic equations of fluid dynamics. Relativistic effects are negligible for the 60.53-MeV center-of-mass initial energy per nucleon considered here. These equations express the conservation of nucleon number, momentum, and energy, for a particular nuclear equation of state. We neglect the surface energy, Coulomb energy, nuclear viscosity, thermal conductivity, and single-particle effects, as well as the production of additional particles and the associated radiative loss of energy from the system.

B. Equations of motion

For our purpose the equations of motion[12] are written conveniently as

$$\frac{\partial n}{\partial t}+\nabla\cdot(n\vec{v})=0\,,$$

$$\frac{\partial(n\vec{v})}{\partial t}+\vec{\nabla}\cdot(n\vec{v}\vec{v})+\frac{1}{m}\vec{\nabla}p=0\,,$$

and

$$\frac{\partial(n)}{\partial t}+\vec{\nabla}\cdot[\vec{v}(n+p)]=0\,.$$

The quantities n, $\mathcal{E}$, and p were defined in Sec. II, and $\vec{v}$ is the velocity of the fluid.

In spherical polar coordinates r, θ, and ϕ, the equations for a spherically symmetric system take the form

$$\frac{Dn}{Dt}+n\left(\frac{\partial v_r}{\partial r}+\frac{2v_r}{r}\right)=0\,,$$

$$\frac{Dv_r}{Dt}+\frac{1}{mn}\frac{\partial p}{\partial r}=0\,,$$

and

$$\frac{D\mathcal{E}}{Dt}+\frac{p}{mn}\left(\frac{\partial v_r}{\partial r}+\frac{2v_r}{r}\right)=0\,,$$

where the Lagrangian time derivative is defined by

$$\frac{D}{Dt}\equiv\frac{\partial}{\partial t}+\vec{v}\cdot\vec{\nabla}\,.$$

For the bound-nucleon mass m we use the mass unit[13]

$$m=931.5016\,\mathrm{MeV}/c^2\,,$$

where c is the speed of light.

C. Numerical solution

It is convenient to solve these equations numerically by means of a Lagrangian-mesh finite-difference technique.[14] We define N spherical fluid cells of constant thickness; the ith cell contains all matter satisfying $r_{i-1}\leqq r<r_i$ ($r_0=0$). The matter in the ith cell is characterized by a particle density n_i and an internal energy per particle $\mathcal{E}_i$. The cell boundaries have velocities v_{i-1} and v_i. With a superscript j denoting the value of a quantity at time $t=j\Delta t$, the finite-difference equations are

$$r_i^j=r_i^{j-1}+v_i^{j-1/2}\Delta t\,,$$

$$n_i^j=n_i^{j-1}\frac{(r_i^{j-1})^3-(r_{i-1}^{j-1})^3}{(r_i^j)^3-(r_{i-1}^j)^3}\,,$$

$$\mathcal{E}_i^j=[\mathcal{E}_i^{j-1}-(\tfrac{2}{3}\mathcal{E}_i^{j-1}+Q_i^{j-1}+Q_i^j)F_i^j\Delta t](1+\tfrac{2}{3}F_i^j\Delta t)^{-1}\,,$$

and

$$v_i^{j+1/2}=v_i^{j-1/2}-4(p_{i+1}^j-p_i^j)\times\Delta t[(r_{i+1}^j-r_{i-1}^j)(n_{i+1}^j+n_i^j)]^{-1}\,,$$

where the pressure

$$p_i^j=n_i^j(Q_i^j+\tfrac{2}{3}\mathcal{E}_i^j)\,,$$

$$Q_i^j=n_i^j\frac{d\mathcal{E}_0(n_i^j)}{dn}-\tfrac{2}{3}\mathcal{E}_0(n_i^j)\,,$$

and

$$F_i^j=\frac{v_i^{j-1/2}-v_{i-1}^{j-1/2}}{r_i^j+r_i^{j-1}-r_{i-1}^j-r_{i-1}^{j-1}}+2\frac{v_i^{j-1/2}+v_{i-1}^{j-1/2}}{r_i^j+r_i^{j-1}+r_{i-1}^j+r_{i-1}^{j-1}}\,.$$

The quantity F_i^j is the finite-difference approximation to $2\vec{\nabla}\cdot\vec{v}$. At the outer edge of the mesh it is necessary to modify the equation for $v_i^{j+1/2}$ to

$$v_N^{j+1/2}=v_N^{j-1/2}+2p_N^j\Delta t\{n_N^j[r_N^j-r_{N-2}^j+\tfrac{1}{2}(r_{N-3}^j-r_{N-1}^j)]\}^{-1}\,.$$

We solve these finite-difference equations with 200 points that are initially equally spaced but that move as the matter expands. The time step is taken to be about 3×10^{-26} s for nonzero values of the compressibility coefficient and about 1×10^{-26} s

for zero compressibility coefficient, corresponding to a perfect gas.

The numerical calculation of the expansion is continued until the density in a cell falls below a freezeout density at which fluid dynamics ceases to be valid.[15-17] For succeeding times, that cell expands with the velocity it had when freezeout occurred. To accomplish this we set the pressure in that cell equal to zero. The time integration is stopped when all the cells have frozen out.

D. Freezeout

Since it is difficult to describe correctly the complicated transition from a fluid to noninteracting nucleons and light nuclei,[15-17] we adopt a two-part criterion for freezeout. First, freezeout is taken to occur if the pressure [Eq. (1)] in a cell becomes zero or negative, which would lead to the formation of clusters even in a fluid-dynamical description. In some cases, the thermal pressure [Eq. (3)] is always larger than the magnitude of the negative compressional pressure, so that the pressure never reaches zero. In this case, freezeout is taken to occur at the density at which the compressional contribution has its maximum negative value. For the equation of state given by Eq. (2) and shown in Fig. 1, this density is $\frac{9}{16} n_0$, a result independent of the value of K. With our initial conditions, this latter criterion governs the freezeout for $K=100$ and 200 MeV. However, for $K=400$ MeV, freezeout occurs when $n \cong 0.75$ n_0 because the total pressure becomes zero at that point.

E. Calculated expansion

Some features of the solution are illustrated in Fig. 2, for a compressibility coefficient equal to 200 MeV. For small values of time, the radial expansion of the matter near the surface is accompanied by a rarefaction wave that propagates inwards through the matter that is initially unaffected. This is similar to the one-dimensional expansion of a semi-infinite compressed perfect gas, for which an analytic solution is possible.[12] However, it is to be contrasted with the analytic solution obtained by Bondorf *et al.*,[18] where the density profile remains rectangular in shape, with a constant decrease in value and expansion of radius. The reason for this is that in the calculations of Bondorf *et al.* the interior thermal energy is not constant but is instead assumed to decrease parabolically with increasing radial distance, reaching zero at the edge. We reproduce to within graphical accuracy the results of Bondorf *et al.* with our numerical calculation when we start with their initial distribution of thermal energy. For larger values of time, our calculated density profile develops a shallow minimum at the center of the nucleus.

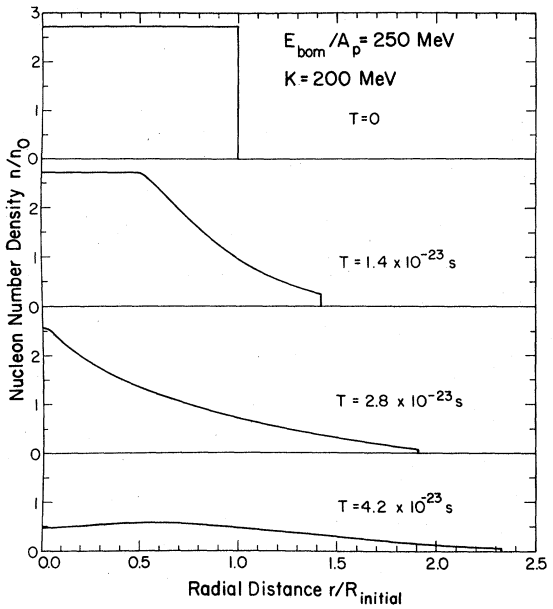

FIG. 2. Time evolution of the density profile for the spherically symmetric expansion of matter that is initially compressed and excited in the head-on collision of an equal target and projectile with a laboratory bombarding energy per nucleon of 250 MeV. The nuclear compressibility coefficient K is 200 MeV. The time scale refers to the expansion of a system with 100 nucleons.

One measure of the accuracy of our numerical calculation is the extent to which energy is conserved. For the case of $K=400$ MeV, the total energy at freezeout is about 0.2% less than the initial energy, whereas for $K=200$ MeV it is about 0.3% less. For the $K=0$ perfect-gas expansion, the final energy is about 1.2% less than the initial energy.

IV. ENERGY DISTRIBUTION OF EXPANDING MATTER

A. Distribution at freezeout

The kinetic-energy distribution $N(E)$ of the expanding matter, normalized to unity when integrated over all energy, is obtained from the basic transformation

$$N(E)\,|dE| = \frac{n(r)4\pi r^2\,|dr|}{A},$$

where the number of nucleons A in the system is related to the initial radius R_i and initial density n_i of the compressed matter by

$$A = \frac{4\pi}{3} R_i^3 n_i .$$

Since the kinetic energy per nucleon at the radius r is given by

$$E(r) = \tfrac{1}{2}mv(r)^2 ,$$

the kinetic-energy distribution becomes

$$N(E) = \frac{3n(r)r^2}{mn_i R_i^3 v(r)\,|dv(r)/dr|} .$$

To evaluate this equation in practice, we represent $n(r)$ and $v(r)$ in the neighborhood of the nearest point r_i by parabolas adjusted to reproduce the values at r_{i-1}, r_i, and r_{i+1}.

We plot in Fig. 3 the resulting kinetic-energy distributions after freezeout for values of the nuclear compressibility coefficient $K = 100$, 200, and 400 MeV. The distributions are very similar, although there is a trend to narrower, higher distributions with increasing K. We also show the kinetic energy distribution for the expansion of a perfect gas, which does not freeze out. In this case, the numerical evolution is continued until the remaining total internal energy of the gas is less than 1% of the initial internal energy. Since the perfect-gas equation of state does not have the −8 MeV per nucleon ground-state energy, this calculation was started with 52.53 MeV of internal energy per nucleon, instead of the 60.53 MeV that was used for the finite-compressibility cases.

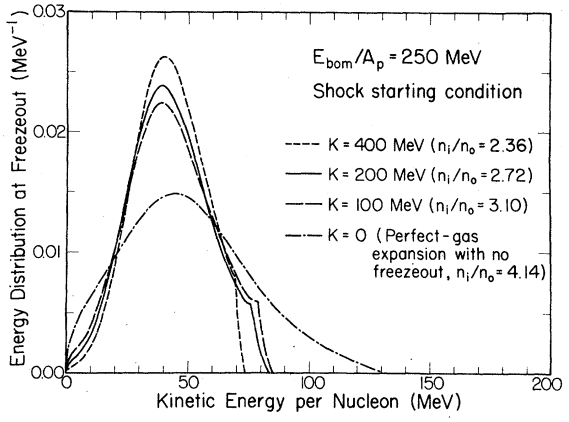

FIG. 3. Distribution of kinetic energy per nucleon after freezeout, for three values of the nuclear compressibility coefficient K, and for the expansion of a perfect gas that is initially compressed and excited with a center-of-mass energy per nucleon of 52.53 MeV.

B. Distribution after thermal folding

At the freezeout point, the expanding matter still contains some thermal energy that contributes to the final energy distribution. To simulate the approximately 8-MeV loss in binding energy per nucleon corresponding to breakup into neutrons and protons rather than composite particles, we measure the remaining thermal energy relative to zero energy rather than relative to the minimum energy at saturation density. We assume that the particles' momenta at freezeout in the reference frame of the moving fluid are distributed according to the nonrelativistic Maxwell-Boltzmann distribution function, with a temperature T equal to $\frac{2}{3}$ of the thermal energy per nucleon (measured with respect to zero energy) divided by the Boltzmann constant k.

The final kinetic-energy distribution $N_f(E)$ is obtained by folding the thermal energy at freezeout into the kinetic-energy distribution at freezeout by means of the relation[19]

$$N_f(E) = \frac{3}{(2\pi mkT)^{1/2}R_i^3}\int_0^{R_{\max}} \frac{n(r)}{n_i}\frac{r^2 dr}{v(r)}\{\exp[-(A-B)^2/kT] - \exp[-(A+B)^2/kT]\},$$

where $A = E^{1/2}$ and $B = \{m[v(r)]^2/2\}^{1/2}$. In the cases that we consider, kT is a constant, since we calculate an isentropic expansion to a constant freezeout density from an initial state with a uniform internal energy distribution. In a more general case, where kT is a function of r, it would need to be included in the integration over r.

After thermal folding, the energy distributions corresponding to $K = 100$, 200, and 400 MeV are indistinguishable from one another to within graphical accuracy, as shown by the solid curve in Fig. 4. However, this common result for nonzero compressibility coefficient peaks at a slightly lower energy and has a longer tail than the dashed curve calculated for zero compressibility coefficient, corresponding to the fluid-dynamical expansion of a perfect gas. Upon comparing with Fig. 3, we see that prior to thermal folding, the energy distributions for nonzero compressibility coefficient are significantly higher and narrower than the distribution for $K = 0$. However, after thermal folding, the results for zero and nonzero compressibility coefficient are only slightly different from each other.

As shown by the dotted line in Fig. 4, the Maxwell-Boltzmann distribution corresponding to entirely thermal energy, which is used in fireball and firestreak models,[17,20,21] peaks at a significantly lower energy and has a longer tail than our calculated solid curve. Finally, the dot-dashed curve

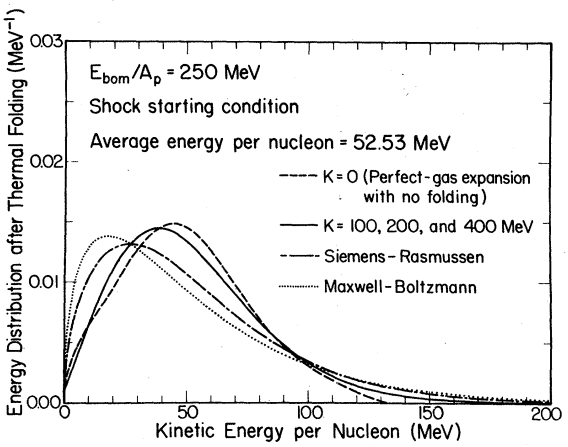

FIG. 4. Distribution of kinetic energy per nucleon after superimposing the thermal energy at freezeout in terms of a nonrelativistic Maxwell-Boltzmann distribution. The results for three values of the nuclear compressibility coefficient K are indistinguishable from one another to within graphical accuracy and are shown by the solid curve, which is compared to three other distributions with the same average energy per nucleon.

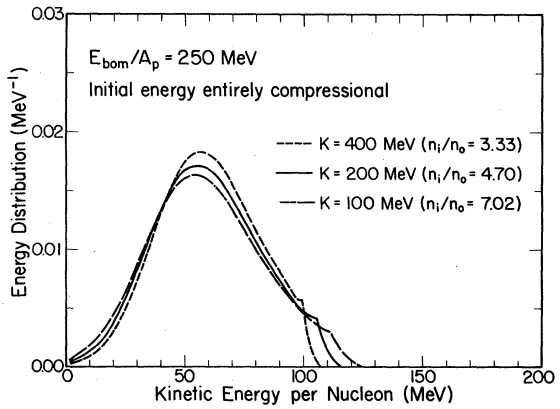

FIG. 5. Distribution of kinetic energy per nucleon after freezeout, for three values of the nuclear compressibility coefficient K, where the starting condition in each case is that all of the collisional energy per nucleon of 60.53 MeV is in compressional energy.

in Fig. 4 is calculated with the Siemens-Rasmussen approximation,[22] which assumes that one-half the initial energy per nucleon appears as constant kinetic energy, with the other half superimposed in terms of a Maxwell-Boltzmann distribution with appropriate nuclear temperature. Although this result is shifted from the pure Maxwell-Boltzmann curve in the correct direction, it still peaks at a lower energy and has a longer tail than our calculated solid curve. This approximation would provide a much better representation of our results if one assumed a uniform kinetic energy per nucleon of about 40 MeV, with the remaining energy thermal, instead of assuming equal amounts of kinetic and thermal energy.

C. Distribution for different initial conditions

In order to see the effects of using initial conditions other than those for a shock-compressed state, we consider finally the case where the initial state corresponds to the center-of-mass energy being converted entirely into compressional energy. The kinetic-energy distributions resulting from these calculations for values of the compressibility coefficient $K = 100$, 200, and 400 MeV are shown in Fig. 5. Although the distributions are somewhat different from those resulting from the shock starting conditions, once again the differences caused by varying the compressibility coefficient in the zero-temperature equation of state are small.

V. CONCLUSIONS

We have integrated numerically the fluid-dynamical equations of motion for the spherically symmetric expansion of nuclear matter that is initially compressed to a density greater than normal nuclear density. For initial conditions we have considered both a shock compressed state with a large amount of thermal energy and a compressed state that contains no thermal energy. In both cases, changing the nuclear compressibility coefficient by a factor of 4 does not greatly alter the final kinetic-energy distribution. In the former case, where some thermal energy remains at freezeout, the superposition of thermal energy and kinetic energy of expansion leads to nearly identical final energy distributions. We conclude that varying the compressibility coefficient in the zero-temperature equation of state does not have an observable effect on the kinetic-energy distribution of expanding matter arising from high-energy heavy-ion collisions.

ACKNOWLEDGMENTS

We have benefited from discussions with J. I. Kapusta, J. W. Negele, and D. Strottman. This work was supported by the U. S. Department of Energy.

[1]A. A. Amsden, G. F. Bertsch, F. H. Harlow, and J. R. Nix, Phys. Rev. Lett. 35, 905 (1975).
[2]F. H. Harlow, A. A. Amsden, and J. R. Nix, J. Comput. Phys. 20, 119 (1976).
[3]A. A. Amsden, F. H. Harlow, and J. R. Nix, Phys. Rev. C 15, 2059 (1977).
[4]J. R. Nix, Prog. Part. Nucl. Phys. 2, 237 (1979).
[5]H. Stöcker, J. A. Maruhn, and W. Greiner, Z. Phys. A 290, 297 (1979).
[6]H. Stöcker, J. A. Maruhn, and W. Greiner, Z. Phys. A 293, 173 (1979).
[7]H. Stöcker, R. Y. Cusson, J. A. Maruhn, and W. Greiner, Z. Phys. A 294, 125 (1980).
[8]P. Danielewicz, Nucl. Phys. A314, 465 (1979).
[9]L. P. Csernai, H. W. Barz, B. Lukács, and J. Zimányi, in *Proceedings of the European Physical Society Topical Conference on Large Amplitude Collective Nuclear Motions, Keszthely, Hungary, 1979* (Central Research Institute for Physics, Budapest, 1979), Vol. II, p. 533.
[10]H. H. K. Tang and C. Y. Wong, Phys. Rev. C 21, 1846 (1980).
[11]W. D. Myers, At. Data Nucl. Data Tables 17, 411 (1976).
[12]F. H. Harlow and A. A. Amsden, Los Alamos Scientific Laboratory Report No. LA-4700, 1971 (unpublished).
[13]T. G. Trippe, A. Barbaro-Galtieri, R. L. Kelly, A. Rittenberg, A. H. Rosenfeld, G. P. Yost, N. Barash-Schmidt, C. Bricman, R. J. Hemingway, M. J. Losty, M. Roos, V. Chaloupka, and B. Armstrong, Rev. Mod. Phys. 48, S1 (1976).
[14]D. Potter, *Computational Physics* (Wiley, London, 1973), pp. 234–236.
[15]A. Mekjian, Phys. Rev. Lett. 38, 640 (1977).
[16]R. Bond, P. J. Johansen, S. E. Koonin, and S. I. A. Garpman, Phys. Lett. 71B, 43 (1977).
[17]J. I. Kapusta, Phys. Rev. C 16, 1493 (1977).
[18]J. P. Bondorf, S. I. A. Garpman, and J. Zimányi, Nucl. Phys. A296, 320 (1978).
[19]J. Terrell, Phys. Rev. 113, 527 (1959).
[20]G. D. Westfall, J. Gosset, P. J. Johansen, A. M. Poskanzer, W. G. Meyer, H. H. Gutbrod, A. Sandoval, and R. Stock, Phys. Rev. Lett. 37, 1202 (1976).
[21]W. D. Myers, Nucl. Phys. A296, 177 (1978).
[22]P. J. Siemens and J. O. Rasmussen, Phys. Rev. Lett. 42, 880 (1979).